Motor imagery performance from calibration to online control in EEG-based brain-computer interfaces

Mahta Mousavi[1] and Virginia R. de Sa[2]

Abstract— **Brain-computer interface (BCI) systems read and infer the user brain activity directly from the brain providing a means of communication and rehabilitation for patients in need. However, brain signals are known to be non-stationary and existing systems are not reliable and robust enough to be taken outside of the laboratory. Often times long calibration and re-calibration of the system is required which can be tiresome and frustrating to the user. In this study, we compare the method of common spatial patterns (CSP) with two of its variants, namely, the canonical correlation analysis approach to common spatial patterns (CCACSP) and the common spatio-spectral patterns (CSSP) in detecting the motor imagery signal when trained on calibration data with sham feedback and tested in online control. We show that the motor imagery performance is significantly better with CSSP and CCACSP compared to CSP and hence, these methods are able to provide a more reliable transfer of the classifier from calibration to online control.**

I. Introduction

Electroencephalography (EEG)-based BCIs are high-speed, non-invasive, inexpensive and portable interventions that enable real-time control of a computer by analyzing electrical brain activity at the scalp [1]. This work focuses on motor imagery BCIs, in which the user imagines moving different parts of her/his body such as the right or left hand or foot, tongue, etc. without actually moving them [2]. Motor imagery BCIs are based on the user's internal, self-initiated patterns of motor imagery. Imagining different body parts results in somewhat different spatial patterns in various frequency bands in the EEG signal [3], [4], [5]. The goal of the BCI is to correctly detect these movement-specific patterns, and translate them into different commands, to allow a user to interact with the world, e.g. to move a prosthetic arm or to move a cursor on a screen.

The viewing of the command to which the BCI output is mapped, i.e., the BCI feedback, can itself modify the state of the user's brain and provide classifiable information [6], [7], [8], [9], [10]. In previous work, we proposed a hybrid BCI to integrate the user brain response to the BCI feedback with the motor imagery classifier [11]. Our results showed significantly better performance compared to a motor imagery BCI that does not use the effect of BCI feedback on the user brain activity. Furthermore, we showed that the trained motor imagery classifier based on the method of common spatial patterns, did not transfer well to the online control as seen in other studies as well [12]. In contrast, we showed that the classifiers trained on the user's brain response to the BCI feedback (that recognized when the BCI made an error) transferred well from calibration to the online control [11].

In this work, we focus on the motor imagery classifier and further study its performance when transferred from calibration to online control. We compare the method of common spatial patterns to two of its variants, namely the canonical correlation analysis approach to common spatial patterns (CCACSP) [13] and the common spatio-spectral patterns (CSSP) [14] in their generalizability from calibration to online control.

II. Methods

A. Experiment

Data were recorded from 12 participants who were naive to BCI (7 females, 1 left-handed, average age = 20.4$\pm$1.0). Prior to their participation, all participants signed an informed consent form that was approved by the Institutional Review Board at UC San Diego. The experiment was comprised of two phases. In the first phase, participants were introduced to motor imagery and performed 30 trials to practice right and left hand motor imagery [15].

In the second phase, participants used right and left hand motor imagery to control a cursor on a screen in front of them. Only the data of the second phase were analyzed in this study. During this phase, in each trial, the cursor appeared at the center of the screen and the target was located three steps away from the cursor to the right or the left. There were a total of 9 blocks in this phase, with 20 trials in each block. In the first 3 blocks, participants were provided with sham feedback but were lead to believe that they were in control of the cursor movements. The recordings of these 3 blocks were used for calibration. The calibrated classifiers were then used in the latter 6 online blocks where the participants actually controlled the movement of the cursor.

Data were recorded using a 64-channel BrainAmp system (Brain Products GmbH) originally at 5000 Hz and downsampled to 100 Hz for analysis. MATLAB [16] and EEGLAB [17] were used to load and epoch the EEG data as well as for plotting. Python was used for stimuli presentation and data analysis during the experiment as well as the offline analysis of the data. For more details about the study please refer to [11].

*This work was supported by NSF IIS 1219200, IIS 1817226, SMA 1041755, and IIS 1528214, FISP G2171, G3155, NIH 5T32MH020002-18 and Mary Anne Fox dissertation year fellowship.

[1]Mahta Mousavi is with the Department of Cognitive Science, UC San Diego, La Jolla, CA 92037, USA mahta@ucsd.edu

[2]Virginia R. de Sa is with the Department of Cognitive Science and the Halıcıoğlu Data Science Institute, UC San Diego, La Jolla, CA 92037, USA desa@ucsd.edu

B. Classification

In the original study [11], three different classifiers were trained on the calibration data: one motor imagery classifier and two error-related brain activity classifiers. In this study, we focus on the right/left hand motor imagery classification of each cursor movement or step.

Data from calibration and online blocks were epoched 0–1 seconds after each cursor movement excluding the last cursor movement. This is because the last cursor movement corresponds to the end of a trial and participants were instructed to stop motor imagery by then. Epochs were filtered in 7-30 Hz with a 6th order Butterworth filter and labelled right/left (R/L) depending on the location of the target.

The original study used the method of common spatial patterns (CSP) for classification of the motor imagery signal during online control. However, in this study, we compare CSP with CCACSP and CSSP in a 'simulated' online fashion. To do so, we used the calibration data to train either of the three methods and tested them on the epoched steps from the online data.

Classifiers were trained and tested in three different conditions: 1) trained and tested on the calibration data using 5-fold cross-validation – called 'calibCV', 2) trained and tested on the online data using 5-fold cross-validation – called 'onlineCV', and 3) trained on the calibration data and tested on the online data – called 'online'.

Right and left steps were balanced in both calibration and online data to avoid challenges in interpretation of the results. After balancing the classes, on average across participants, there were a total of 136 and 272.7±38.4 steps in the calibration and online blocks, respectively [11]. All 64 channels were used for classification.

Next we will briefly summarize the methods under study.

C. Common Spatial Patterns (CSP)

The method of common spatial patterns (CSP) [3], [5] is widely used for feature extraction in motor imagery BCI.

Let $X_{ij} \in \mathbb{R}^{C\times T}$ be the $j-th$ bandpassed EEG data epoch over C channels with T time samples that belongs to class $i \in \{1,2\}$. Let classes 1 and 2 be the two motor imagery classes (e.g., the movement imagination of the right and left hands). The covariance for each class $i \in \{1,2\}$ is estimated as follows:

$$\Sigma_i = \frac{1}{N}\sum_{j=1}^{N}\frac{X_{ij}X_{ij}^T}{tr(X_{ij}X_{ij}^T)}, \tag{1}$$

where N is the population of each class. In our analysis, we balanced the population of classes by subsampling the more populated class. This is further explained later.

CSP finds a set of filters that maximizes the variance for one class while minimizing it for the other by solving the following optimization problem:

$$\arg\max_{w} \quad \frac{w^T\Sigma_1 w}{w^T(\Sigma_1+\Sigma_2)w}. \tag{2}$$

Combining the above for both classes provides the CSP filters which are the eigenvectors corresponding to the largest and smallest eigenvalues of the following:

$$\Sigma_1 w = \lambda(\Sigma_1+\Sigma_2)w. \tag{3}$$

We selected the top 3 CSP filters for each class. Features were selected as the logarithm of the variance of the filtered epochs through the selected 6 filters. Linear discriminant analysis (LDA) with automatic shrinkage [18] was then trained on the selected features.

D. Canonical Correlation Analysis Approach to Common Spatial Patterns (CCACSP)

The CSP method considers spatial features of the signal and ignores potential relevant temporal features. The canonical correlation analysis approach to common spatial patterns (CCACSP) [13] generalizes CSP to consider the temporal aspects of the signal as well.

Let $X_{ij} \in \mathbb{R}^{C\times T}$ be the $j-th$ bandpassed epoch corresponding to class $i \in \{1,2\}$. Define $X_{ij}^{(-1)} \in \mathbb{R}^{C\times T}$ and $X_{ij}^{(+1)} \in \mathbb{R}^{C\times T}$, similarly, representing the one-sample backward and forward time-shifted epochs, respectively. The time-shifted covariance for class i is estimated as follows:

$$\Sigma_{Si} = \frac{1}{N}\sum_{j=1}^{N}\frac{X_{ij}(X_{ij}^{(-1)}+X_{ij}^{(+1)})^T}{tr(X_{ij}(X_{ij}^{(-1)}+X_{ij}^{(+1)})^T)}, \tag{4}$$

CCACSP combines ideas from canonical correlation analysis (CCA) and CSP by solving the following set of optimization problems:

$$\begin{aligned}\arg\max_{w} \quad & \frac{w^T\Sigma_{S1}w}{w^T(\Sigma_1+\Sigma_2)w}\\ \arg\max_{v} \quad & \frac{v^T\Sigma_{S2}v}{v^T(\Sigma_1+\Sigma_2)v}\end{aligned} \tag{5}$$

The solutions, also called the CCACSP filters, are the eigenvectors associated with the following generalized eigenvalue problems:

$$\begin{aligned}\Sigma_{S1}w &= \lambda(\Sigma_1+\Sigma_2)w\\ \Sigma_{S2}v &= \lambda(\Sigma_1+\Sigma_2)v\end{aligned} \tag{6}$$

We selected the top 3 CCACSP filters for each class resulting in a total of 6 selected filters. Features were selected as the logarithm of the variance of the filtered epochs through the selected 6 filters. A linear discriminant analysis (LDA) with automatic shrinkage [18] was then trained on the selected features.

The code for CCACSP can be found here: `https://github.com/mahtamsv/CCACSP`.

E. Common Spatio-Spectral Patterns (CSSP)

This method was proposed as a variant of the CSP method that is capable of extracting robust and invariant features [14].

Let $X_{ij} \in \mathbb{R}^{C\times T}$ be the $j-th$ bandpassed epoch corresponding to class $i \in \{1,2\}$. CSSP finds the set of filters W and W^τ such that the variance of the filtered epochs

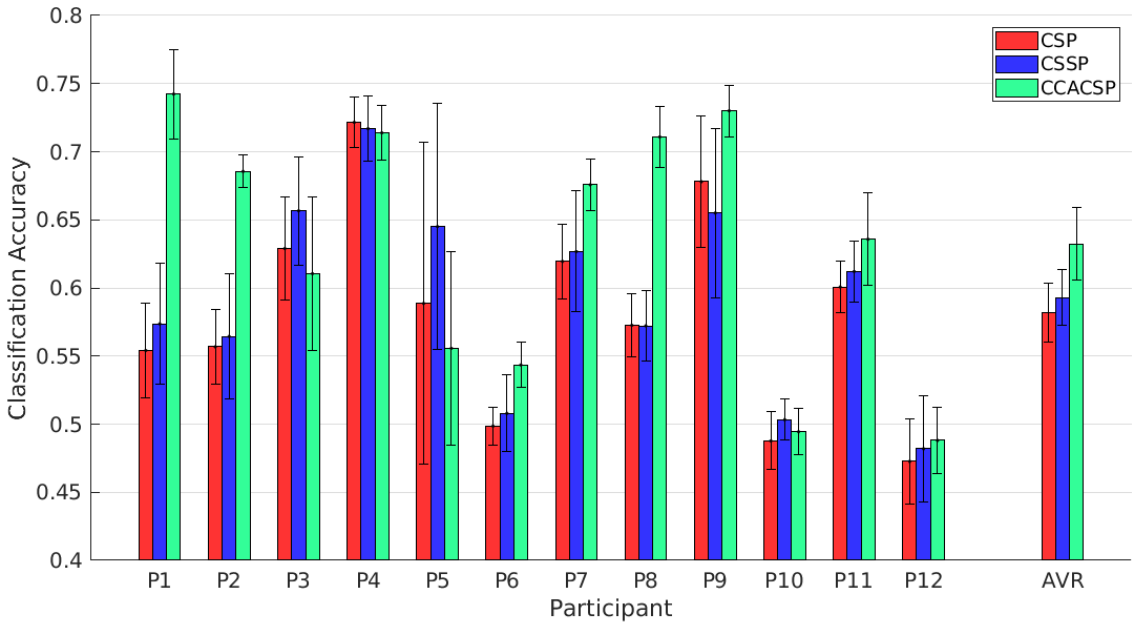

Fig. 1: Comparison of the R/L motor imagery classification accuracy when trained on calibration and tested on the online data with CSP, CSSP and CCACSP. The red, blue and green bars are also presented in the last columns of Tables I, II and III, respectively.

$Z_j = WX_j + W^{(\tau)}X_j^{(\tau)}$ – where $X_j^{(\tau)}$ is the τ time-shifted version of X_j – is maximized for one class while minimized for the other class and vice versa.

Define a new epoch by concatenating each epoch with its time-shifted version as follows:

$$\hat{X}_j = \begin{pmatrix} X_j \\ X_j^{(\tau)} \end{pmatrix} \tag{7}$$

By applying CSP to these newly defined epochs, one finds $\hat{W}$ which can be divided into two submatrices W and W^τ.

The top and bottom 3 filters for each class from W and W^τ were selected and called W_s $W_s^\tau$and , epochs were filtered as $W_sX_j + W_s^{(\tau)}X_j^{(\tau)}$ and the logarithm of the variance of the filtered epochs were selected as features. A linear discriminant analysis (LDA) with automatic shrinkage [18] was then trained on the selected features.

Note that the hyper-parameter τ was trained using cross-validation on the training data in the range 0–15 as suggested by the authors in [14].

III. Results

Tables I, II and III show the performance of the R/L classifier on previously recorded EEG data with CSP, CCACSP and CSSP under the 3 conditions stated earlier. Since balancing the right and left classes was done by randomly subsampling the larger class 10 times, the first number for each participant shows the average across the 10 instances of balanced classes and the second number is the standard deviation. For the last row, 'AVR' indicates the average across participants where the first number is the mean and the second number is the standard error.

Across participants, CCACSP online performance is significantly better than the CSP online performance (Wilcoxon signed rank test, $p = 0.027$) and similarly, CSSP online performance is significantly better than the CSP online performance (Wilcoxon signed rank test, $p = 0.043$). But the difference between CCACSP online performance and CSSP online performance is not significant (Wilcoxon signed rank test, $p = 0.13$). For easier visualization, the online performance or transferred accuracy (last columns of Tables) of the three methods are also presented as bar plots in Figure 1.

Note that the performance of the R/L classifier with CSP in calibCV or onlineCV (middle two columns in Tables I,II, and III) is not different from CCACSP nor CSSP (Wilcoxon signed rank test, $p > 0.06$). This shows the calibration to online generalization efficacy of the CSSP and CCACSP methods compared to the CSP method. In effect, the CSSP and CCACSP methods find classifiers that generalize better from calibration to online control.

IV. Discussion

Non-stationarity in brain activity limits the generalization of the classifiers trained on calibration data to the online control (test data) [12], [11]. In this work, we compared the performance of the motor imagery classifier with the commonly used CSP with two of its variants: CCACSP and CSSP. In previous work, we showed that CSP performance was significantly affected when trained on calibration and tested during online control. In this work, we showed that using CSSP [14] and CCACSP [13] could serve as a solution to alleviate this issue and result in improved online motor

TABLE I: R/L classifier with **CSP**.

ID	calibCV	onlineCV	online
P1	0.73/0.02	0.84/0.02	0.55/0.03
P2	0.74/0.02	0.70/0.02	0.56/0.03
P3	0.75/0.02	0.78/0.05	0.63/0.04
P4	0.87/0.03	0.72/0.02	0.72/0.02
P5	0.79/0.05	0.81/0.03	0.59/0.12
P6	0.60/0.05	0.57/0.02	0.50/0.01
P7	0.63/0.06	0.77/0.04	0.62/0.03
P8	0.67/0.04	0.70/0.04	0.57/0.02
P9	0.81/0.04	0.73/0.02	0.68/0.05
P10	0.73/0.04	0.65/0.02	0.49/0.02
P11	0.81/0.03	0.64/0.05	0.60/0.02
P12	0.67/0.04	0.59/0.02	0.47/0.03
AVR	0.73/0.02	0.71/0.02	0.58/0.02

TABLE II: R/L classifier with **CSSP**.

ID	calibCV	onlineCV	online
P1	0.72/0.03	0.83/0.03	0.57/0.04
P2	0.72/0.05	0.71/0.02	0.56/0.05
P3	0.76/0.03	0.75/0.05	0.66/0.04
P4	0.87/0.03	0.72/0.02	0.72/0.02
P5	0.78/0.05	0.78/0.03	0.65/0.09
P6	0.59/0.03	0.58/0.02	0.51/0.03
P7	0.61/0.04	0.76/0.03	0.63/0.04
P8	0.68/0.04	0.70/0.04	0.57/0.03
P9	0.79/0.04	0.71/0.03	0.66/0.06
P10	0.72/0.03	0.63/0.02	0.50/0.02
P11	0.81/0.04	0.62/0.04	0.61/0.02
P12	0.67/0.03	0.59/0.02	0.48/0.04
AVR	0.73/0.02	0.70/0.02	0.59/0.02

TABLE III: R/L classifier with **CCACSP**.

ID	calibCV	onlineCV	online
P1	0.74/0.03	0.82/0.02	0.74/0.03
P2	0.66/0.03	0.70/0.02	0.69/0.01
P3	0.74/0.04	0.77/0.04	0.61/0.06
P4	0.86/0.03	0.75/0.03	0.71/0.02
P5	0.58/0.07	0.65/0.04	0.56/0.07
P6	0.58/0.05	0.60/0.02	0.54/0.02
P7	0.63/0.05	0.75/0.02	0.68/0.02
P8	0.72/0.04	0.69/0.04	0.71/0.02
P9	0.83/0.03	0.75/0.02	0.73/0.02
P10	0.69/0.04	0.54/0.02	0.49/0.02
P11	0.79/0.01	0.61/0.06	0.64/0.03
P12	0.65/0.04	0.53/0.03	0.49/0.02
AVR	0.71/0.03	0.68/0.03	0.63/0.03

imagery performance. In comparing CCACSP with CSSP, we see that the CSSP mean is closer to the CSP mean, but there is larger variability in the CCACSP results.

As future work, we will investigate better ways to extract temporal information by emphasizing relevant sources. We hope that by doing so, the gap in motor imagery performance from calibration to online control will be reduced and the overall BCI performance improved.

REFERENCES

[1] L. F. Nicolas-Alonso and J. Gomez-Gil, "Brain computer interfaces, a review," *Sensors*, vol. 12, no. 2, pp. 1211–1279, 2012.

[2] G. Pfurtscheller and C. Neuper, "Motor imagery and direct brain-computer communication," *Proceedings of the IEEE*, vol. 89, no. 7, pp. 1123–1134, 2001.

[3] H. Ramoser, J. Muller-Gerking, and G. Pfurtscheller, "Optimal spatial filtering of single trial EEG during imagined hand movement," *IEEE Transactions on Rehabilitation Engineering*, vol. 8, no. 4, pp. 441–446, 2000.

[4] G. Pfurtscheller, C. Brunner, A. Schlögl, and F. L. Da Silva, "Mu rhythm (de) synchronization and EEG single-trial classification of different motor imagery tasks," *NeuroImage*, vol. 31, no. 1, pp. 153–159, 2006.

[5] B. Blankertz, R. Tomioka, S. Lemm, M. Kawanabe, and K.-R. Muller, "Optimizing spatial filters for robust EEG single-trial analysis," *IEEE Signal Processing Magazine*, vol. 25, no. 1, pp. 41–56, 2008.

[6] A. S. Koerner and V. R. de Sa, "A novel method to integrate error detection into motor imagery BCI," in *Workshop on Brain-Machine Body Interfaces, 34th Annual International Conference of the IEEE Engineering in Medicine and Biology Society*. IEEE, 2012.

[7] A. S. Koerner, Q. Zhang, and V. R. de Sa, "The effect of real-time positive and negative feedback on motor imagery performance," in *the International BCI Meeting*, 2013. [Online]. Available: http://dx.doi.org/10.3217/978-3-85125-260-6-73

[8] T. O. Zander, L. R. Krol, N. P. Birbaumer, and K. Gramann, "Neuroadaptive technology enables implicit cursor control based on medial prefrontal cortex activity," *Proceedings of the National Academy of Sciences*, vol. 113, no. 52, pp. 14 898–14 903, 2016.

[9] R. Chavarriaga, A. Sobolewski, and J. d. R. Millán, "Errare machinale est: the use of error-related potentials in brain-machine interfaces," *Frontiers in Neuroscience*, vol. 8, p. 208, 2014.

[10] M. Mousavi, A. S. Koerner, Q. Zhang, E. Noh, and V. R. de Sa, "Improving motor imagery BCI with user response to feedback," *Brain-Computer Interfaces*, vol. 4, no. 1-2, pp. 74–86, 2017.

[11] M. Mousavi, L. R. Krol, and V. de Sa, "Hybrid brain-computer interface with motor imagery and error-related brain activity," *Journal of Neural Engineering*, 2020.

[12] P. Shenoy, M. Krauledat, B. Blankertz, R. P. Rao, and K.-R. Müller, "Towards adaptive classification for BCI," *Journal of Neural Engineering*, vol. 3, no. 1, p. R13, 2006.

[13] E. Noh and V. R. De Sa, "Canonical correlation approach to common spatial patterns," in *2013 6th International IEEE/EMBS Conference on Neural Engineering (NER)*. IEEE, 2013, pp. 669–672.

[14] S. Lemm, B. Blankertz, G. Curio, and K.-R. Muller, "Spatio-spectral filters for improving the classification of single trial EEG," *IEEE transactions on biomedical engineering*, vol. 52, no. 9, pp. 1541–1548, 2005.

[15] M. Mousavi and V. R. de Sa, "Towards elaborated feedback for training motor imagery brain computer interfaces," in *Proceedings of the 7th Graz Brain-Computer Interface Conference 2017*, 2017, pp. 332–337.

[16] MATLAB and S. T. R. 2018b. Natick, Massachusetts, United States: The MathWorks Inc., 2018.

[17] A. Delorme and S. Makeig, "EEGLAB: an open source toolbox for analysis of single-trial EEG dynamics including independent component analysis," *Journal of Neuroscience Methods*, vol. 134, no. 1, pp. 9–21, 2004.

[18] O. Ledoit and M. Wolf, "Honey, I shrunk the sample covariance matrix," *The Journal of Portfolio Management*, vol. 30, no. 4, pp. 110–119, 2004.